Nuclear Engineering and Technology 51 (2019) 1871–1885

Contents lists available at ScienceDirect

Nuclear Engineering and Technology

journal homepage: www.elsevier.com/locate/net

Original Article

Application of TULIP/STREAM code in 2-D fast reactor core high-fidelity neutronic analysis

Xianan Du [a], Jiwon Choe [a], Sooyoung Choi [a], Woonghee Lee [a], Alexey Cherezov [a], Jaeyong Lim [b], Minjae Lee [b], Deokjung Lee [a, *]

[a] Department of Nuclear Engineering, Ulsan National Institute of Science and Technology (UNIST), 50 UNIST-gil, Ulsan, 44919, Republic of Korea
[b] Korea Atomic Energy Research Institute, 111 Daedeok-Daero 989 beon-gil, Yuseong-gu, Daejeon, Republic of Korea

ARTICLE INFO

Article history:
Received 28 February 2019
Received in revised form
20 May 2019
Accepted 8 June 2019
Available online 10 June 2019

Keywords:
TULIP
STREAM
Fast reactor
MOC core calculation

ABSTRACT

The deterministic MOC code STREAM of the Computational Reactor Physics and Experiment (CORE) laboratory of Ulsan National Institute of Science and Technology (UNIST), was initially designed for the calculation of pressurized water reactor two- and three-dimensional assemblies and cores. Since fast reactors play an important role in the generation-IV concept, it was decided that the code should be upgraded for the analysis of fast neutron spectrum reactors. This paper presents a coupled code - TULIP/STREAM, developed for the fast reactor assembly and core calculations. The TULIP code produces self-shielded multi-group cross-sections using a one-dimensional cylindrical model. The generated cross-section library is used in the STREAM code which solves eigenvalue problems for a two-dimensional assembly and a multi-assembly whole reactor core. Multiplication factors and steady-state power distributions were compared with the reference solutions obtained by the continuous energy Monte-Carlo code MCS. With the developed code, a sensitivity study of the number of energy groups, the order of anisotropic P_N scattering, and the multi-group cross-section generation model was performed on the k_{eff} and power distribution. The 2D core simulation calculations show that the TULIP/STREAM code gives a k_{eff} error smaller than 200 pcm and the root mean square errors of the pin-wise power distributions within 2%.

1. Introduction

For decades the conventional two-step approach to the assembly transport calculation and core diffusion/transport calculation has been applied in thermal reactor and fast reactor core design. During the two-step calculation, one important thing is to generate accurate few-group cross sections through a homogenization routine. With the improved understanding of the physical mechanism of neutron transport, the high-fidelity/one-step neutronic calculation has attracted a lot of attention from researchers. Unlike the conventional two-step approach, the one-step calculation is committed to the direct whole-core calculation with a heterogeneous assembly model and it can obtain accurate results with higher pin-wise resolution. Several deterministic codes have been employed by various institutions, such as CRX [1], DeCART [2], nTRACER [3], MPACT [4], NECP-X [5] and STREAM [6]. In addition, the APOLLO3 [7], EXUS-F/nTRACER [8], and MC^2-3/PROTEUS [9,10] codes aim to perform high-fidelity whole-core calculation in fast reactor (FR) field.

The STREAM (Steady state and Transient REactor Analysis with Method of characteristic) code has been developed by the Computational Reactor Physics and Experiment laboratory (CORE) of Ulsan National Institute of Science and Technology (UNIST). It was initially designed for pressurized water reactor (PWR) assembly calculations and its 3-D calculation capabilities have been verified in a recent study [11]. With the development of the next generation-IV reactor design, FR will play a very important role and meanwhile, the accurate numerical simulations of FR with pin-wise resolution will be necessary. Therefore, it is worthwhile to make an extension of the STREAM code to perform the FR neutronic calculation. The primary study of the STREAM code on fast reactor

* Corresponding author. Department of Nuclear Engineering, Ulsan National Institute of Science and Technology, 50 UNIST-gil, Ulsan, 44919, Republic of Korea.
E-mail addresses: dxndxnwww@unist.ac.kr (X. Du), chi91023@unist.ac.kr (J. Choe), schoi@unist.ac.kr (S. Choi), dldndgml0310@unist.ac.kr (W. Lee), alcher@unist.ac.kr (A. Cherezov), limjy@kaeri.re.kr (J. Lim), lmj@kaeri.re.kr (M. Lee), deokjung@unist.ac.kr (D. Lee).

https://doi.org/10.1016/j.net.2019.06.010

analysis was performed in April 2018 [12]. In that study, pin-cell and assembly problems were analyzed with a library with different ultrafine groups. Due to the lack of resonance treatment, 300–500 pcm differences were found even though a 2082-group library was used. To continue the work, the generation of accurate ultrafine-group cross sections should be considered in the STREAM code.

The TULIP [13] code was developed by the Nuclear Engineering Computational Physics (NECP) laboratory at Xi'an Jiaotong University. It was designed for FR ultrafine- and few-group self-shielded cross sections generation. Since then, the TULIP code has been embedded in the SARAX [14] code system for FR core neutronic analysis and the verification and validation of SARAX code system have been performed in recent studies [15].

In the FR neutronic analysis, it is quite meaningful to obtain results with pin-wise resolution. Due to the inclined radial flux gradient in the fuel-blanket interface, the depletion calculation in blanket region will lose accuracy with nodal averaged flux. Although pin-wise power reconstruction can obtain approximated power distribution in blanket region, the reference high-fidelity pin-wise results are necessary. In addition, the reactivity feedback due to thermal expansion is important during the operation, especially in some transient situation. The high-fidelity calculation with explicit geometry description can treat thermal expansion of the fuel, cladding, coolant, and duct separately by coupling with thermal-hydraulic and fuel performance calculation. In order to solve those problems and get best understanding of Gen-IV FR core or other advanced core design, the high-fidelity FR calculation with directly method of characteristics (MOC) transport solver was launched. Since both TULIP and STREAM code have been verified against various problems, coupling those two codes should be an effective way to perform high-fidelity FR core neutron analysis.

To start the work, there are still some fundamental issues that should be investigated. To perform the whole-core calculation, the pin-wise self-shielded cross sections should be obtained first. The proper geometry model for the resonance calculation should be determined to balance the accuracy and efficiency. What is more, thousands of energy groups and higher order of anisotropic scattering matrices require more memory and computational time, especially for the whole-core calculation. It would be meaningful to reduce the number of energy groups and order of anisotropic scattering matrices during the whole-core simulation with adequate accurate results.

In this paper, the TULIP and STREAM code are coupled for the 2-D core calculation. The next section briefly describes the theory of TULIP/STREAM code. Section 3 describes how the sensitivity studies were performed based on the assembly calculation. Section 4 and Section 5 summarize the results of the 2-D rectangular and hexagonal pseudo core problems, respectively. Section 6 gives the conclusion to close the paper.

2. Description of simulation code

2.1. TULIP/STREAM

The TULIP code applies the method of directly self-shielding the point-wise (PW) cross sections from PENDF data based on the ENDF/B-VII.0 [16] library. The homogeneous and heterogeneous 1-D cylinder/slab problems can be solved to obtain self-shielded cross sections. The computational flow chart of the TULIP code is shown in Fig. 1.

To begin with, the TULIP code gets the geometry and composition information from the input file. If a 1-D problem needs to be solved, the escape cross sections for each region and isotope are calculated using Tone's method [17]. In the unresolved resonance (URR) energy range, an additional interpolating table is given in a PENDF file, which is a function of the background cross section, energy, and temperature. Then, the self-shielded cross sections in URR for a specific composition can be obtained by interpolation of the background cross section. For the resolved resonance (RR) energy range, the average total, fission, and total elastic scattering cross sections in each ultrafine group can be calculated through the numerical integration of Eq. (1). The neutron flux is obtained based on narrow resonance (NR) approximation. The TULIP code applies 1968 ultrafine energy group structure, which is same as the ECCO code.

$$\overline{\sigma}_{x,g} = \frac{\int_{\Delta E_g} \sigma_x(E)\phi(E)dE}{\int_{\Delta E_g} \phi(E)dE} \tag{1}$$

where, $\mathscr{X}$ stands for reaction type and g stands for the energy group.

When self-shielded total elastic scattering cross sections are determined, each order of scattering matrices can be calculated using the scattering function, which only depends on the isotope and energy group structure. For other information, such as non-elastic scattering matrices (including inelastic scattering matrices and (n,2n) reaction), neutron fission spectrum, and neutron release per fission, the cross sections are prepared in ultrafine group form using the NJOY [18] code. After performing ultrafine group transport calculation and homogenization, the final self-shielded cross sections can be obtained. Finally, the TULIP code would output ultrafine and final self-shielded cross sections in decimal format.

The STREAM code uses the MOC for transport and it adopts several methods and functions for PWR modeling, for instance, the pin-based pointwise energy slowing-down method for resonance treatment, the sub-channel thermal-hydraulic calculation, and the source term calculation. The Tabuchi-Yamamoto quadrature set with three polar angle divisions is used for the polar angle discretization [19]. In addition, the STREAM code can perform the transport calculation with input macroscopic cross sections. Moreover, the hexagonal MOC transport solver was adopted in the STREAM code recently. In the code, the hexagonal-assembly based modular ray tracing kernel was implemented [20]. Therefore, the STREAM code has the capability of analyzing different type of FR.

Since the neutron behaviors in FR are totally different from those in thermal reactor and the resonance calculation module in STREAM is not designed for FR, a new module for FR cross sections calculation should be invoked in STREAM. Therefore, the TULIP code is coupled with the STREAM code for FR neutronic analysis. The aim of this work is to perform whole-core transport calculation with explicit geometry modeling. In the TULIP/STREAM code system, the resonance calculation is performed by the TULIP code to prepare self-shielded cross sections for individual materials such as the fuel, cladding, coolant, and duct by considering the local heterogeneity effects. Whole-core MOC transport calculations are performed by STREAM to obtain the multiplication factor and pin-wise power distribution.

2.2. MCS Monte Carlo code

MCS [21] is a 3-D continuous-energy code for particle transport based on the Monte Carlo method. It was also developed by the CORE group at UNIST. The code currently handles neutron and photon transport and is designed for two major classes of problem related to nuclear reactor physics:

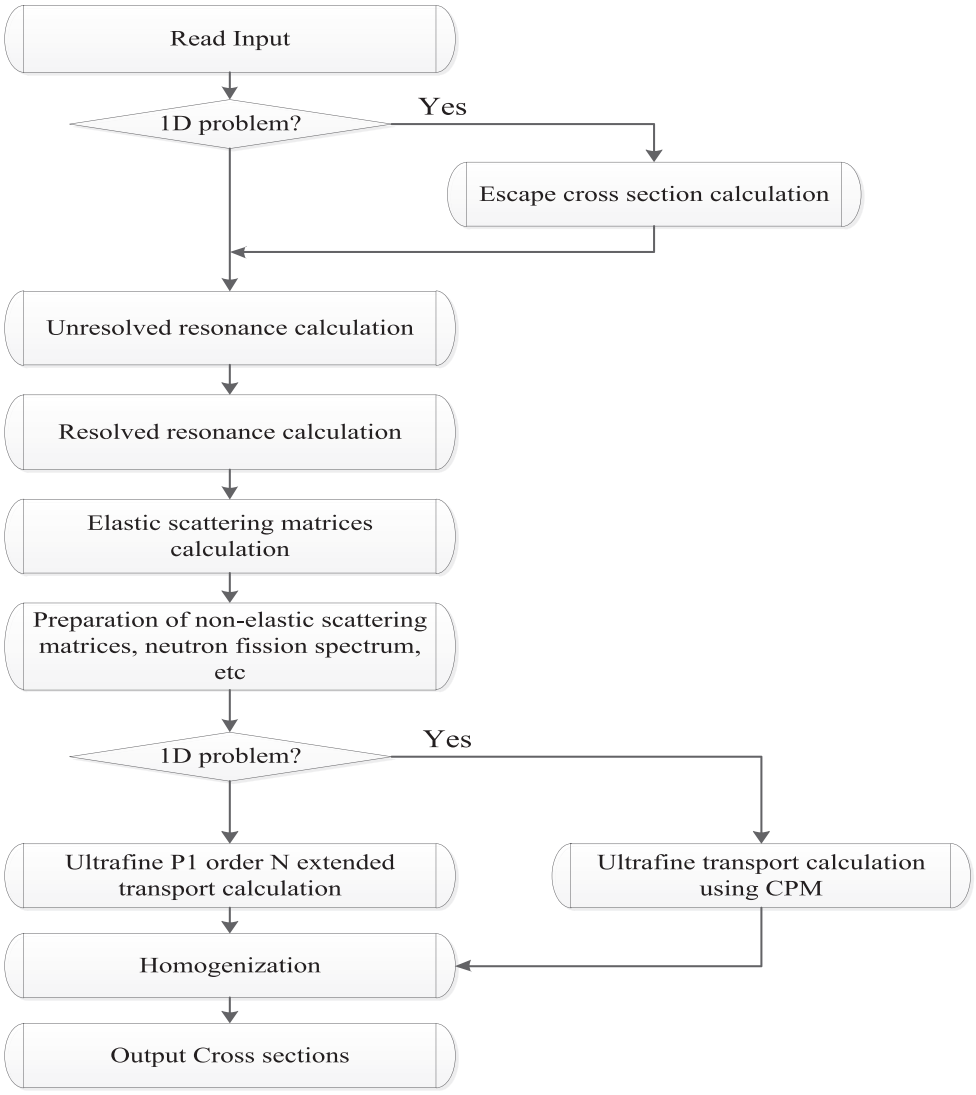

Fig. 1. The computational flow chart of TULIP code.

- Criticality problems, with or without coupling with external physics codes (fuel performance/thermal-hydraulics) and with or without depletion;
- Radiation shielding problems (propagation of fixed sources in multiplying or non-multiplying media).

The method introduction and verifications of the MCS code have been accomplished in the recent studies. In those studies, the MCS results agreed well with other mainstream Monte Carlo codes, such as Serpent. Therefore, in this paper, the reference solution is obtained with MCS code. Only the ENDF/B-VII.0 library would be used during the simulation to make sure the results were consistent with the TULIP/STREAM calculation.

3. Sensitivity analysis based on assembly problem

In this section, a sensitivity analysis of the calculation condition is discussed, specifically the energy group, order of scattering, the selection of angular discretization and ray distance, and the selection of the cross section generation model. The design of the PASCAR [22] (Proliferation-resistant Accident-tolerant Self-supported, Capsular and Assured Reactor) reactor, developed by Seoul National

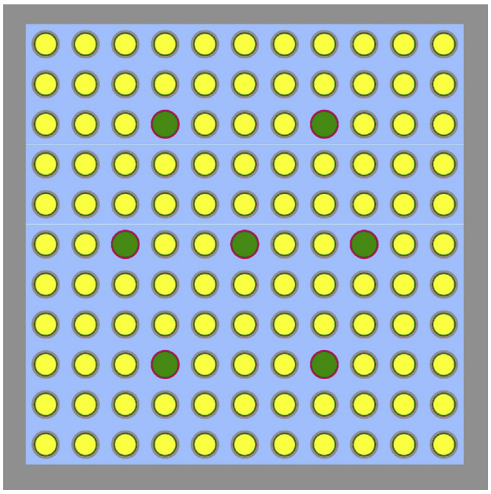

Fig. 2. Geometry of assembly problem.

Table 1
Assembly problem specification.

Pin	Material	Radius, cm	Nuclide
Fuel	(U, Pu) Zr	0.32606	U, Np, Pu, Am, *Cm*, Zr (U–Pu: Inner 6.35%/Outer 9.38%)
	Pb	0.36384	Pb
	Zr	0.37399	Zr
	HT-9	0.45000	Cr, Mn, Fe, Ni, Mo
	LBE	–	Pb, Bi
Structure	Pb	0.40500	Pb
	Zr	0.45500	Zr

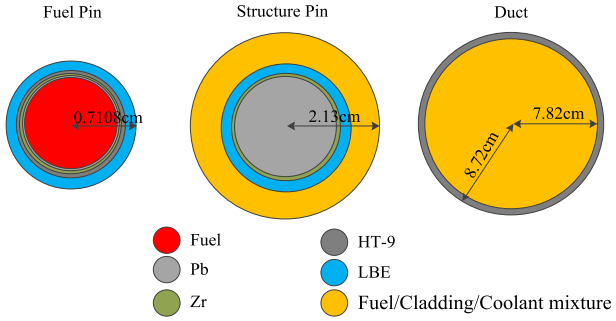

Fig. 3. Geometry specification of type-wise model.

University, was adopted in the sensitivity analysis.

3.1. Description of geometry and composition

The PASCAR reactors consist of rectangular fuel assemblies, unlike the usual fast reactors which consist of hexagonal fuel assemblies. Based on their design, the assembly consisting of 11 × 11 pins is analyzed in the following sections. Fig. 2 shows the geometry of the assembly. In total, 114 fuel pins and 7 structure pins are in one assembly. The fuel pin is loaded with (U, Pu) Zr metallic fuel with lead-bismuth (LBE) as the coolant material. The cladding consists of 3 rings made with different kind of materials. On the outside of assembly, there is 8 mm thick duct made of HT-9. The boundary condition is reflective and the pin pitch is 1.26 cm. Two fuel assemblies with different Pu enrichment are calculated in this paper. The specifications of the assembly are shown in Table 1.

3.2. Numerical result

To prepare the cross sections for each pin, two models were used, the type-wise model and ring-wise model. In the type-wise model, the cross sections were calculated for each kind of pin, including fuel pin, structure pin, and duct. The geometry for the calculation is shown in Fig. 3. The volume of each model equals that of 1 pin, and 9 pins and assembly, respectively. The cross sections would only depend on the type.

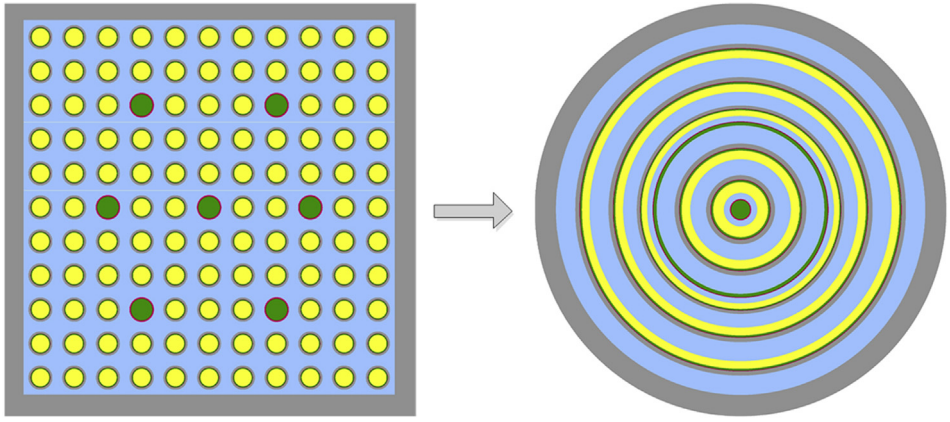

Fig. 4. Geometry specification of ring-wise model.

Table 2
Summary of k_{eff} results of Inner fuel assembly.

Code	Group	Scattering	XS model	k_{eff}	Diff., pcm	Time, s	Memory, GB
MCS	CE			1.01043 ± 0.00003		34032[a]	1.143
TULIP STREAM	1968	P0	Ring-wise	1.01195	152	7378	7.648
		TR		1.01115	72	7378	7.648
		P0	Type-wise	1.01463	420	7637	7.116
		TR		1.01384	341	6562	7.116
		P1		1.01361	318	354840	10.000
		P2		1.01403	360	501261	10.300
		P3		1.01387	344	772949	10.700
	195	P0	Ring-wise	1.01204	161	386	0.459
		TR		1.01137	94	408	0.459
		P0	Type-wise	1.01598	555	412	0.425
		TR		1.01529	486	298	0.425
		P1		1.01519	476	2152	0.430
		P2		1.01554	511	3268	0.435
		P3		1.01540	497	4620	0.440

[a] Equivalent 1 cpu simulation time.

Table 3
Summary of k_{eff} results of Outer fuel assembly.

Code	Group	Scattering	XS model	k_{eff}	Diff., pcm	Time, s	Memory, GB
MCS	CE			1.17520 ± 0.00003		34154[1]	1.143
TULIP STREAM	1968	P0	Ring-wise	1.17664	144	7220	7.648
		TR		1.17588	68	8066	7.648
		P0	Type-wise	1.17913	393	6582	7.116
		TR		1.17837	317	6289	7.116
		P1		1.17815	295	352918	10.000
		P2		1.17854	334	539273	10.300
		P3		1.17839	319	832670	10.700
	195	P0	Ring-wise	1.17666	146	400	0.459
		TR		1.17601	81	388	0.459
		P0	Type-wise	1.18059	539	328	0.425
		TR		1.17994	474	335	0.425
		P1		1.17984	464	2183	0.430
		P2		1.18017	497	3141	0.435
		P3		1.18004	484	4322	0.440

1: equivalent 1 cpu simulation time.

Table 4
Results of sensitivity test of ray distance and angular discretization.

Ray distance, cm	Azimuthal angle	12	24	48	64	96
0.03		1.01227	1.01024	1.01112	1.01121	1.01137
0.05		1.01231	1.01024	1.01112	1.01117	1.01137

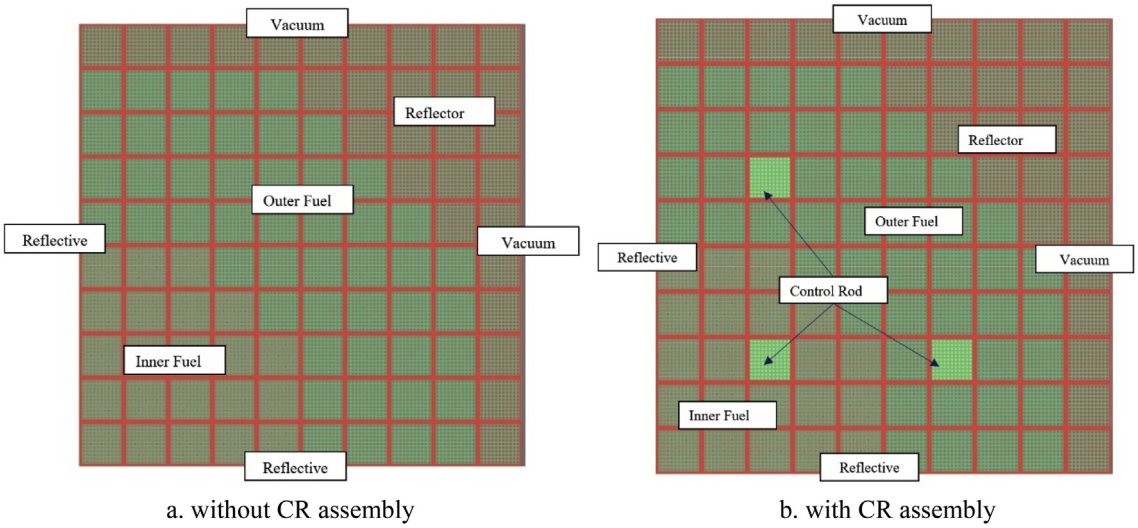

Fig. 5. The layout of 2-D pseudo core problems.

Fig. 4 shows the geometry specification of the ring-wise model. The square assembly can be divided into 8 rings. For example, the first ring only contains one structure pin. Therefore, in the ring-wise model, there would be 3 rings to model one structure pin based on the geometry of the structure pin. It should be note that, in the square assembly, the distance from the center to each pin in the same ring varies. In this way, it differs from the natural ring-wise hexagonal assembly. In order to get accurate self-shielded cross sections, the spatial distribution of different material needs to be described in the resonance calculation. Considering the long mean free path, an approximation was made that the contribution of the spatial material distribution in the resonance calculation is more important than that of the distance. Therefore, for the 8 fuel pins in the next ring, a cylindrical geometry with the same volume was built, even though each pin has a different distance from the center. Following the rule of conservation of volume, the ring-wise model can be built. The cross sections for pins in each ring would be the same when the using ring-wise model. When using the ring-wise model, the cross sections depend on not only the pin type, but also location of the pin, such as in the center of the assembly or near the duct.

To perform the calculation, 1968-group self-shielded cross sections were prepared by the TULIP code. In order to reduce the time consumption of the transport calculation, 195-group cross sections were also used in the calculation. The 195-group cross sections were condensed by solving the 1968-group 1-D cylinder problem

Table 5
Nuclide density of B_4C.

Isotope	Nuclide density, $\times 10^{24}$
C12	2.70e-02
B10	2.32e-02
B11	8.49e-02

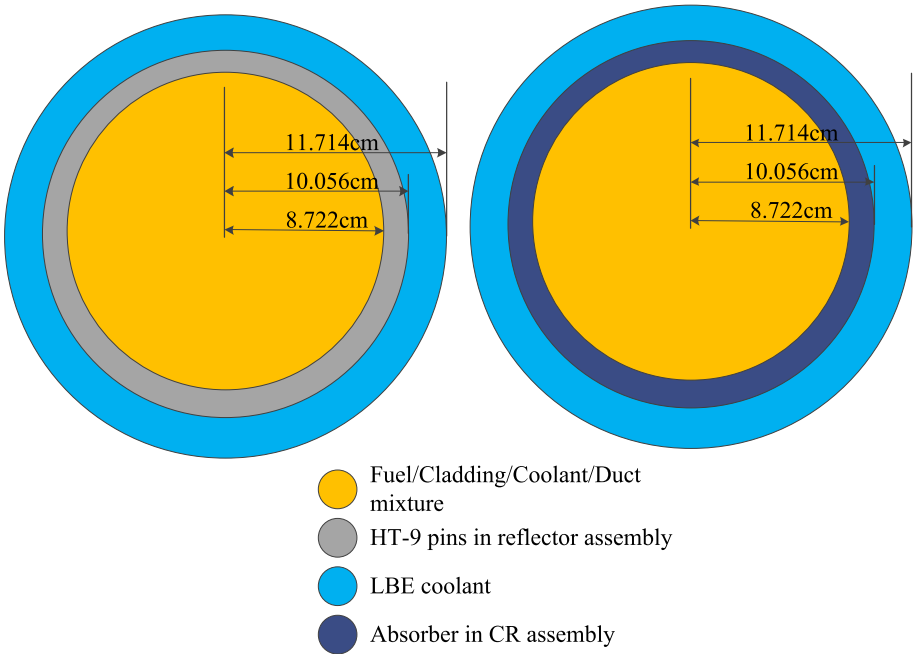

Fig. 6. 1-D super-assembly model for reflector/absorber pin cross section generation.

Table 6
Summary of k_{eff} value for the core without CR assembly.

	k_{eff}	Diff, pcm	Simulation time, min
Reference	1.01426 ± 0.00002		17360[1]
Case 1, P0, OP1	1.02839	1354	244
Case 2, TR, OP1	1.01626	194	243
Case 3, TR, OP2	1.01565	135	246

1: equivalent 1 cpu simulation time.

with CPM. The energy group structure of the 195-group is based on 1968 groups. On average, each coarse group contains 10 energy groups. In addition, the TULIP code prepared P0, P1, P2, P3 and transport correction (TR) scattering transfer cross sections for the STREAM code.

The STREAM MOC transport calculation was performed with a 0.03 cm ray distance and 96 azimuthal angles, which were rigorous conditions. The reference solution was obtained with a MCS

0.611 0.628 2.72%	0.598 0.615 2.78%	0.570 0.587 2.92%	0.524 0.539 2.88%	0.466 0.477 2.37%					MCS TULIP/STREAM Rel.diff
0.942 0.968 2.80%	0.925 0.952 2.95%	0.887 0.915 3.12%	0.824 0.851 3.34%	0.728 0.752 3.26%	0.625 0.640 2.42%				
1.194 1.218 2.01%	1.178 1.203 2.13%	1.141 1.171 2.61%	1.077 1.109 2.99%	0.973 1.005 3.30%	0.828 0.856 3.33%	0.678 0.694 2.42%			
1.335 1.338 0.26%	1.324 1.331 0.55%	1.300 1.315 1.16%	1.254 1.280 2.03%	1.165 1.198 2.84%	1.020 1.054 3.29%	0.828 0.856 3.34%	0.625 0.640 2.43%		
1.109 1.082 -2.48%	1.106 1.083 -2.05%	1.102 1.089 -1.21%	1.347 1.354 0.52%	1.289 1.313 1.83%	1.165 1.198 2.87%	0.972 1.005 3.37%	0.728 0.752 3.32%	0.466 0.477 2.42%	
1.111 1.059 -4.67%	1.111 1.064 -4.21%	1.111 1.075 -3.25%	1.112 1.094 -1.59%	1.346 1.354 0.57%	1.254 1.280 2.07%	1.076 1.109 3.09%	0.823 0.851 3.45%	0.523 0.539 3.04%	
1.110 1.040 -6.32%	1.111 1.047 -5.76%	1.112 1.059 -4.76%	1.111 1.075 -3.24%	1.101 1.089 -1.11%	1.299 1.315 1.21%	1.141 1.171 2.66%	0.887 0.915 3.19%	0.570 0.586 2.86%	
1.108 1.027 -7.30%	1.109 1.034 -6.78%	1.111 1.047 -5.74%	1.111 1.064 -4.20%	1.105 1.083 -2.01%	1.323 1.331 0.60%	1.177 1.203 2.22%	0.924 0.952 3.03%	0.598 0.615 2.87%	
1.106 1.020 -7.79%	1.107 1.027 -7.26%	1.110 1.040 -6.30%	1.111 1.059 -4.66%	1.109 1.082 -2.44%	1.334 1.338 0.29%	1.193 1.218 2.05%	0.941 0.968 2.86%	0.611 0.628 2.84%	

Fig. 7. Assembly-wise radial power distribution and relative difference of Case 1.

0.611	0.598	0.570	0.524	0.466				MCS
0.618	0.605	0.576	0.529	0.472				TULIP/STREAM
1.09%	1.11%	0.99%	0.97%	1.29%				Rel.diff
0.942	0.925	0.887	0.824	0.728	0.625			
0.944	0.927	0.890	0.826	0.732	0.632			
0.25%	0.25%	0.30%	0.30%	0.52%	1.14%			
1.194	1.178	1.141	1.077	0.973	0.828	0.678		
1.193	1.177	1.141	1.077	0.974	0.833	0.685		
-0.08%	-0.07%	-0.02%	0.02%	0.12%	0.56%	1.09%		
1.335	1.324	1.300	1.254	1.165	1.020	0.828	0.625	
1.332	1.321	1.297	1.253	1.164	1.022	0.833	0.632	
-0.19%	-0.20%	-0.22%	-0.12%	-0.08%	0.15%	0.56%	1.15%	
1.109	1.106	1.102	1.347	1.289	1.165	0.972	0.728	0.466
1.106	1.102	1.099	1.343	1.287	1.164	0.974	0.732	0.472
-0.31%	-0.33%	-0.30%	-0.29%	-0.19%	-0.05%	0.18%	0.57%	1.35%
1.111	1.111	1.111	1.112	1.346	1.254	1.076	0.823	0.523
1.106	1.106	1.107	1.108	1.343	1.253	1.077	0.826	0.529
-0.44%	-0.43%	-0.37%	-0.34%	-0.24%	-0.08%	0.12%	0.42%	1.12%
1.110	1.111	1.112	1.111	1.101	1.299	1.141	0.887	0.570
1.104	1.105	1.107	1.107	1.099	1.297	1.141	0.890	0.576
-0.55%	-0.53%	-0.45%	-0.36%	-0.20%	-0.17%	0.03%	0.37%	1.10%
1.108	1.109	1.111	1.111	1.105	1.323	1.177	0.924	0.598
1.101	1.103	1.105	1.106	1.102	1.321	1.177	0.927	0.604
-0.62%	-0.56%	-0.52%	-0.42%	-0.29%	-0.15%	0.01%	0.33%	1.03%
1.106	1.107	1.110	1.111	1.109	1.334	1.193	0.941	0.611
1.100	1.101	1.104	1.106	1.106	1.332	1.193	0.944	0.618
-0.55%	-0.58%	-0.53%	-0.43%	-0.28%	-0.16%	-0.04%	0.31%	1.20%

Fig. 8. Assembly-wise radial power distribution and relative difference of Case 2.

0.611	0.598	0.570	0.524	0.466				MCS
0.611	0.598	0.570	0.524	0.467				TULIP/STREAM
-0.06%	-0.06%	-0.06%	0.02%	0.22%				Rel.diff
0.942	0.925	0.887	0.824	0.728	0.625			
0.941	0.924	0.886	0.823	0.729	0.628			
-0.07%	-0.08%	-0.15%	-0.06%	0.10%	0.50%			
1.194	1.178	1.141	1.077	0.973	0.828	0.678		
1.193	1.177	1.141	1.076	0.973	0.830	0.681		
-0.08%	-0.07%	-0.02%	-0.07%	0.02%	0.19%	0.50%		
1.335	1.324	1.300	1.254	1.165	1.020	0.828	0.625	
1.334	1.323	1.299	1.254	1.165	1.021	0.830	0.628	
-0.04%	-0.05%	-0.07%	-0.04%	0.01%	0.05%	0.20%	0.51%	
1.109	1.106	1.102	1.347	1.289	1.165	0.972	0.728	0.466
1.109	1.106	1.102	1.346	1.289	1.165	0.973	0.729	0.467
-0.04%	0.03%	-0.03%	-0.07%	-0.04%	0.03%	0.08%	0.16%	0.28%
1.111	1.111	1.111	1.112	1.346	1.254	1.076	0.823	0.523
1.111	1.110	1.111	1.111	1.346	1.254	1.076	0.823	0.524
0.01%	-0.07%	-0.01%	-0.07%	-0.02%	0.00%	0.03%	0.05%	0.17%
1.110	1.111	1.112	1.111	1.101	1.299	1.141	0.887	0.570
1.109	1.110	1.112	1.111	1.102	1.299	1.141	0.886	0.570
-0.10%	-0.08%	0.00%	0.00%	0.07%	-0.02%	0.03%	-0.08%	0.05%
1.108	1.109	1.111	1.111	1.105	1.323	1.177	0.924	0.598
1.107	1.108	1.110	1.110	1.106	1.323	1.177	0.924	0.598
-0.08%	-0.11%	-0.07%	-0.06%	0.07%	0.00%	0.01%	0.00%	0.03%
1.106	1.107	1.110	1.111	1.109	1.334	1.193	0.941	0.611
1.106	1.107	1.109	1.111	1.109	1.334	1.193	0.941	0.611
-0.01%	-0.03%	-0.08%	0.02%	-0.01%	-0.01%	-0.04%	-0.01%	0.05%

Fig. 9. Assembly-wise radial power distribution and relative difference of Case 3.

simulation, which used 100 inactive batches, 500 active batches, and 300000 particles per batch neutron history.

Table 2 and Table 3 summarize the TULIP/STREAM results compared to the MCS solutions. According to these results, the ring-wise cross-sections generation model obtained more accurate results. Because one assembly calculation with reflective boundary condition was performed, the results under P0 approximation are closer to references. The relative differences between the TULIP/STREAM P0 calculation and MCS are around 140–160 pcm. When transport correction was implemented, the results improved by 80 pcm. However, when much higher order scattering matrices were considered, the results were not much improved, but the memory cost and time consumption increased a lot. Compared to the results that were obtained with 1968-group calculation, when ring-wise model was implemented, the 195-group calculation did not lose too much accuracy. The difference between the 1968-group and 195-group calculation is less than 30 pcm.

In order to investigate the convergence of k_{eff} when the MOC calculation conditions change, the inner fuel assembly was calculated again. In these calculations, 0.03 and 0.05 cm ray distances were selected while the azimuthal angle from 12 to 96 were chosen. The results are summarized in Table 4. As shown, about a 200 pcm difference in the k_{eff} could be found between the 12 and 24 azimuthal angles. When the number of angles increases to 48 or more, the k_{eff} becomes converged. On the other hand, the results show that due to the long mean free path, a big ray distance can be selected for fast reactor calculation.

4. PASCAR 2-D pseudo core problem

4.1. Description and modeling of core

In this section, two 2-D pseudo cores were calculated to verify the accuracy of the TULIP/STREAM code system for whole-core calculation. Fig. 5 shows the layout of the quarter 2-D pseudo cores. The first core only consists of the inner fuel assembly, outer fuel assembly and reflector assembly. The composition and geometry of the inner and outer fuel assembly are the same as the assembly mentioned in the previous sections. There are 121 HT-9 pins in the reflector assembly and the diameter of each pin is 0.91 cm. Similarly to the fuel assembly, the reflector assembly has a HT-9 duct with a thickness of 8 mm. Meanwhile, there are three control rod (CR) assemblies in the second core. The geometry of the CR assembly is the same as the reflector assembly but the composition of each pin is B_4C. The nuclide density of each isotope is shown in Table 5.

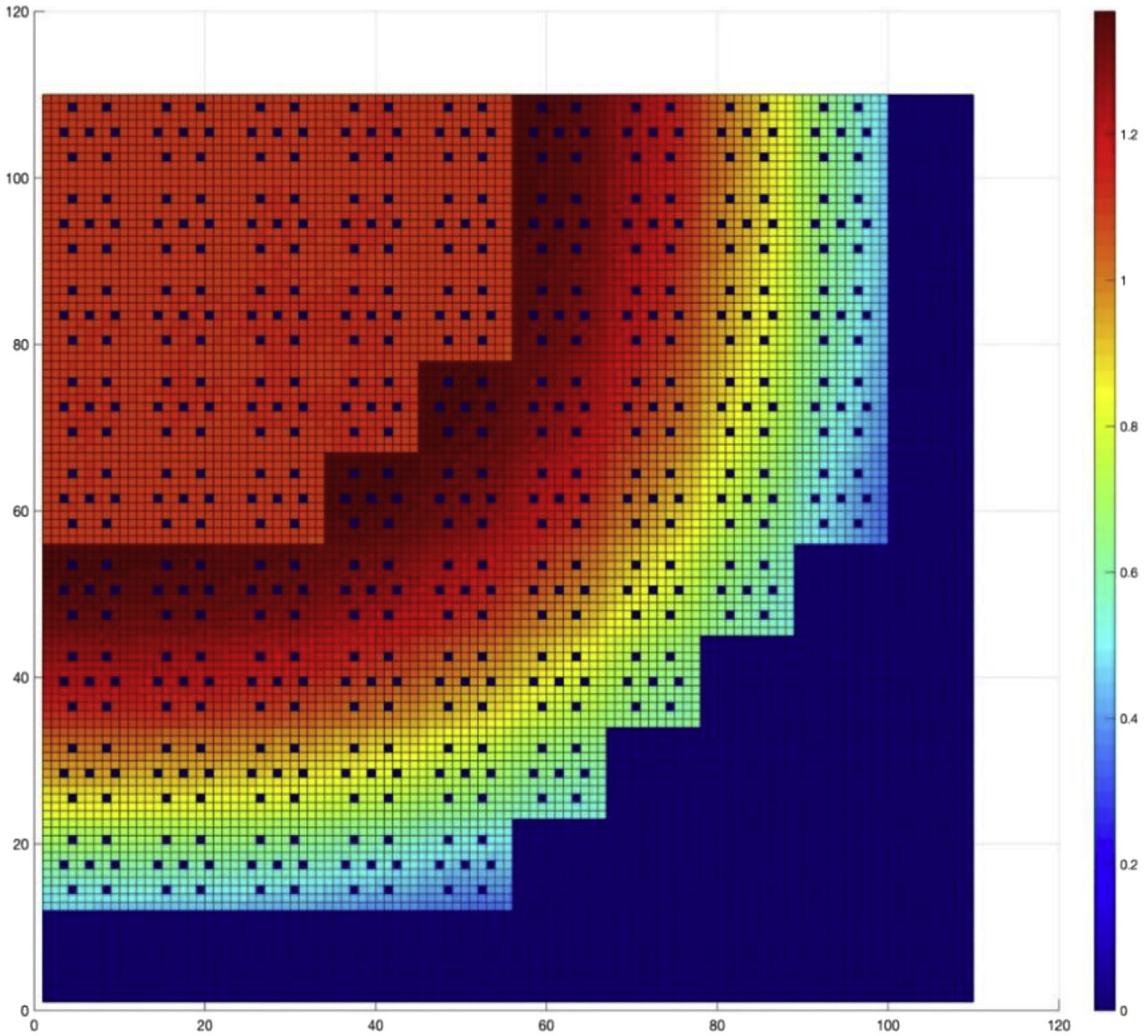

Fig. 10. Pin-wise power distribution obtained with MCS reference calculation.

The best approach to achieve the whole-core calculation would be to generate cross sections based on whole-core explicit geometry. However, it would cost a lot of memory to save each pin's cross sections. In addition, the resonance calculation would be difficult finished due to the excessive computational time. Therefore, in the 2-D core calculation, the self-shielded cross sections are prepared based on different kinds of assembly.

According to the previous results, the ring-wise assembly model can give more accurate results. So, the cross sections for each pin of the inner and outer fuel assembly is calculated with the ring-wise assembly model. To obtain cross sections for non-fuel assembly, such as reflector HT-9 pin, two options were selected and compared. For the first option (OP1), the cross sections of reflector HT-9 pin were calculated using homogeneous model. For the second option (OP2), a 1-D super-assembly model was built, which is shown in Fig. 6. This 1-D super-assembly model was applied for both reflector assembly and CR assembly.

In the center of the 1-D super-assembly model, the fuel, cladding, coolant, and duct materials are homogenized into one mixture based on one fuel assembly. The volume of second ring equals to that of 121 HT-9/B_4C pins while the volume of third ring equals to the coolant in the assembly.

4.2. Analysis of 2-D core without CR assembly

In this section, three cases were simulated to investigate the factor that affects the accuracy of the whole-core calculation. For both Case 1 and Case 2, the reflector pin cross sections were obtained with model OP1. The difference was that Case 1 performed P0 calculation while Case 2 implemented transport correction to consider the anisotropic scattering. Different from Case 2, the model for reflector pin in Case 3 was based on OP2. The macroscopic cross sections for each composition were prepared in 195 multigroup form. Each MOC calculation applied the condition with a 0.05 cm ray distance and 48 azimuthal angles. 100 inactive batches, 1000 active batches, and 600000 particles per batch neutron history were used in the MCS simulation to obtain reference k_{eff} and assembly/pin-wise power distribution.

Table 6 summarizes the k_{eff} value compared to the reference. Differently from the assembly calculation, a large difference can be found between the P0 calculation and the reference. It is reasonable in the core calculation due to the neutron leakage. When the anisotropic scattering was considered, the accuracy increased a lot. Less than 200 pcm relative difference exists between Case 2 and the reference. Compared to Case 2, Case 3 used a more detailed model for reflector pin cross section generation, so that the accuracy of the k_{eff} value continued to increase. The TULIP/STREAM calculation took about 250 min to finish one simulation in total.

Fig. 7 to Fig. 9 show the assembly-wise power distribution and relative difference of each case. Case 1 shows a bad result, which is consistent with the k_{eff} result. The largest negative difference is −7.79% at the inner core region. Even for the outer core assembly with only around 0.6 relative power, the difference is still more than 2.4%. As the results show in Fig. 8 of Case 2, the power distribution agrees well with reference solution. The differences are from −0.62% to 1.35% and the RMS is 0.57%, which is much smaller

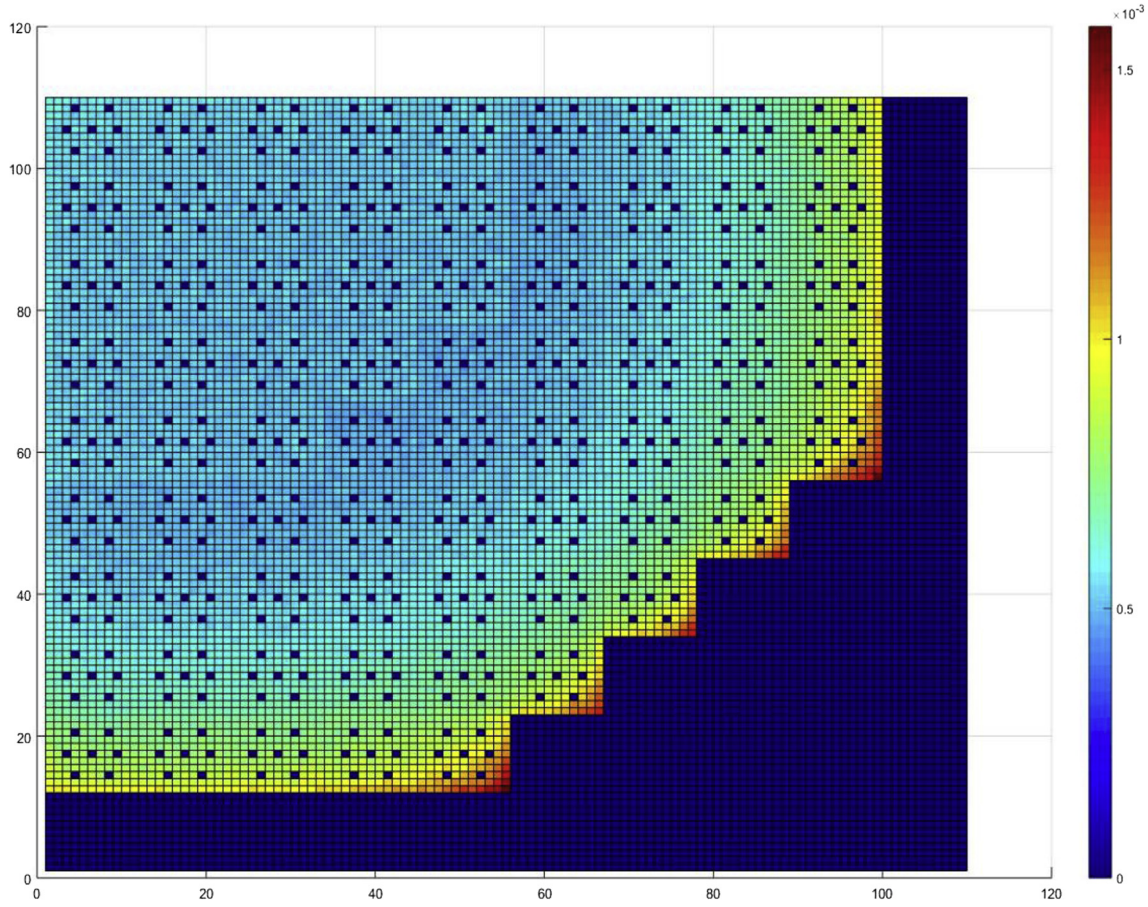

Fig. 11. Standard deviation of pin-wise power distribution obtained with MCS.

than that of Case 1. But assemblies that are located outside the core still have more than 1% difference compared to the references. This is due to the inaccurate cross section generation model of reflector pins. When the 1-D super-assembly model was used to generate reflector pin cross sections, the results of the power distribution became closer compared to the reference solution. The maximum relative difference is 0.51% while the minimum is −0.11%. The RMS is only 0.13%. Based on the k_{eff} and power distribution results, the 1-D super-assembly model improves the accuracy remarkably.

The comparison under pin-wise resolution is more important when performing whole-core calculations with explicit geometry. Therefore, Fig. 10 shows the pin-wise power distribution obtained with the MCS simulation and Fig. 11 shows its standard deviation. Fig. 12 and Fig. 13 show the relative difference of the power distribution. Since Case 1 has huge differences in assembly-wise power distribution, the comparison of pin-wise power is only made between Case 2, Case 3 and the references.

It can be found from Fig. 10 that the power distribution at the inner core region was quite flat. The standard deviation of pin-wise power tally was around 0.0005 relative value, which is acceptable. Compared to the references, the largest relative differences exist at the interface between the outer fuel assembly and reflector assembly in both Case 2 and Case 3. The value is 2.14% in Case 2 while 1.08% in Case 3. Clearly, the implementation of the 1-D super-assembly model increases the accuracy of the pin-wise power distribution, especially at the interface regions. Due to the more accurate pin-wise power distribution, the RMS decreased from 0.69% to 0.27%.

4.3. Analysis of 2-D core with CR assembly

The 2-D core with CR assembly is analyzed in this section. Based on the results of the previous section, ring-wise model for fuel assembly, the 1-D super-assembly model for non-fuel assembly and TR calculation will get most the accurate results. Therefore, those options would be used to verify the accuracy of TULIP/STREAM with the strong neutron absorber. In the same way as in the case of no-CR, a 0.05 cm ray distance and 48 azimuthal angles were applied in the MOC calculation. The reference calculation was still performed by running the MCS code with 100 inactive batches, 1000 active batches, and 600000 particles per batch neutron history.

The k_{eff} results are shown in Table 7. The pin-wise power distribution obtained with MCS and the relative difference between TULIP/STREAM and MCS are shown in Fig. 14 and Fig. 15, respectively. Although there are several neutron absorber assemblies located in the core, only 159 pcm differences can be found in k_{eff} value compared to the reference. Due to neutron absorption, the pin power decreases near the CR assembly. In addition, the TULIP/STREAM code can get an accurate estimation of the pin-wise power distribution for the core with CR assembly. The maximum relative difference is 1.3%, which still exists at the interface between the outer fuel assembly and reflector assembly. The relative powers of those pins are from 0.6 to 0.8. The RMS is only 0.32%, which indicates that the TULIP/STREAM code system can be applied in both

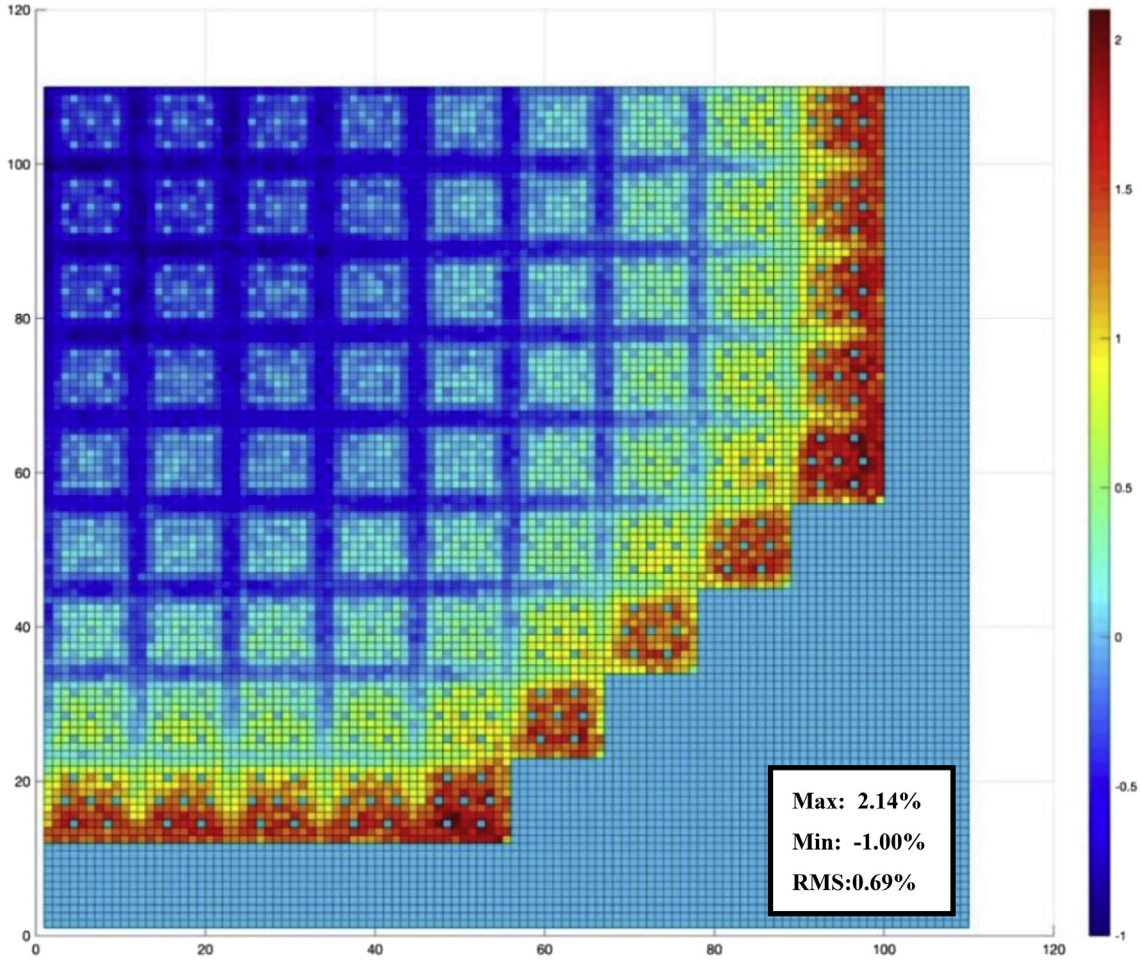

Fig. 12. Relative difference of pin-wise power distribution between Case 2 and MCS, unit in %.

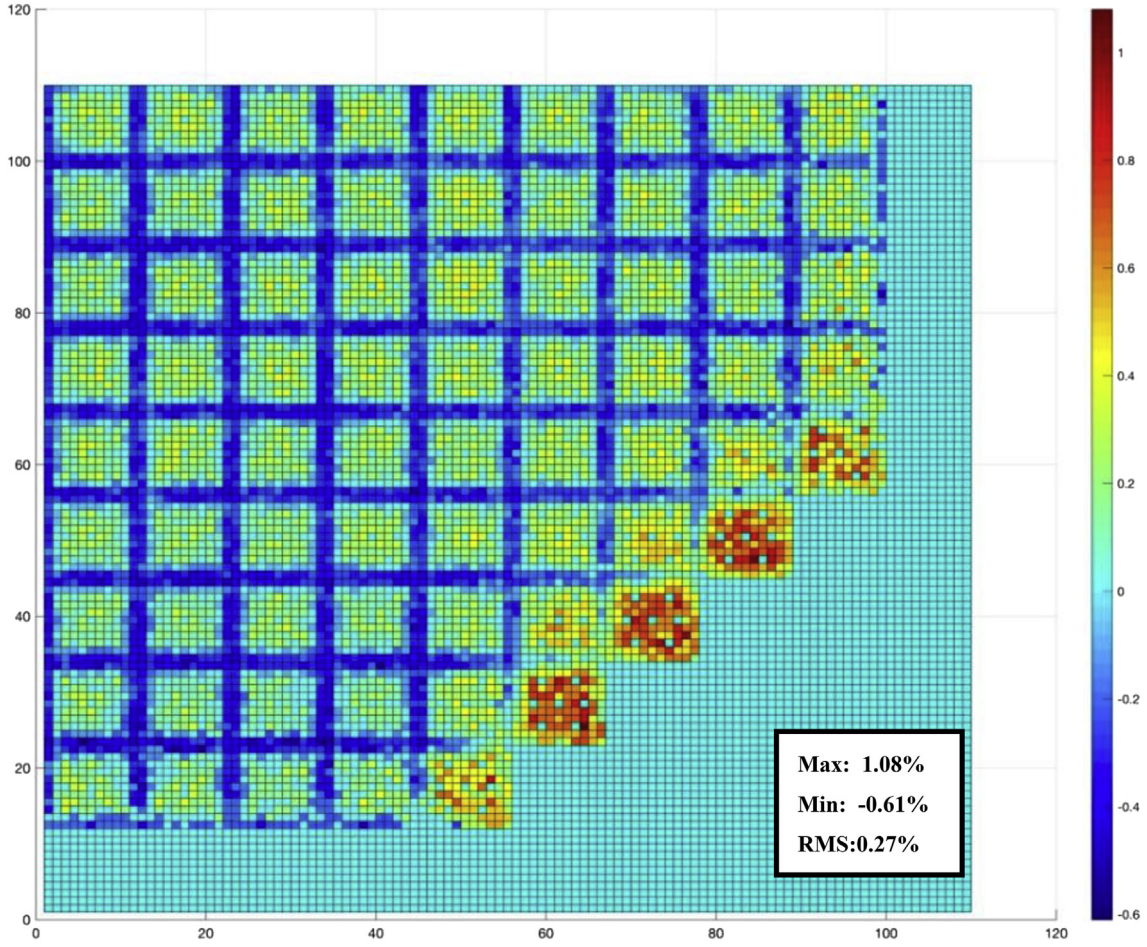

Fig. 13. Relative difference of pin-wise power distribution between Case 3 and MCS, unit in %.

Table 7
Summary of keff value for the core with CR assembly.

	k_{eff}	Diff., pcm
Reference	0.90206 ± 0.00002	
TULIP/STREAM	0.90336	159

CR in and CR out core calculation.

5. MET-1000 2-D pseudo core problem

5.1. Problem description

In this section, two 2-D pseudo core problems (Case A and Case B) based on the MET-1000 numerical benchmark [23] were selected to verify the accuracy with hexagonal geometry. The layout of each case is shown in Fig. 16. Six different kinds of assembly were considered in the calculation: an Inner Fuel assembly, Outer Fuel assembly, Control Rod assembly, Radial Reflector assembly, Radial Shielding assembly and Empty Duct assembly. Among these assembly types, only the Inner Fuel, Outer Fuel, and Control Rod assembly were considered as heterogeneous model. The geometry and composition of each assembly were same as in the reference document [23].

In order to perform verification, four cases in total were calculated, namely the Case A and Case B nominal state, Case B sodium voided (SV) state, and Case B Doppler state. For the nominal states, the temperature of the fuel and structural material were set as 800 K and 700 K, respectively. For the Case B SV state, the nuclide density of ^{23}Na in the fuel assembly region was set as 1.0e20 since the current STREAM code cannot deal with voided regions. For the Case B Doppler state, the fuel temperature was increased to 1600 K.

5.2. Numerical result

The whole-core calculation was performed with the TULIP/STREAM code. According to the results of Section 3 and Section 4, the ring-wise model and super-assembly model were used to generate the self-shielded cross sections of different assemblies. Due to the large number of flat source regions, the whole-core calculation would cost a large amount of computational time. Therefore, in this section, along with 195-group cross sections, 33-group cross sections were also prepared by the TULIP code. The outflow transport correction was used to take the anisotropic scattering into account. The STREAM MOC transport calculation was performed with 0.05 cm ray distance and 24 azimuthal angles. The reference calculation was performed by the MCS code with the neutron history of 100 inactive cycles, 1000 active cycles, and 200,000 particles per cycle.

Table 8 summarizes the k_{eff} value of the verifications. Fig. 17 shows the relative power distribution of the Case A and Case B nominal state obtained with the MCS code. Fig. 18, Fig. 19 and Table 9 show the relative differences of power distribution and their Max./Min./RMS value in each case.

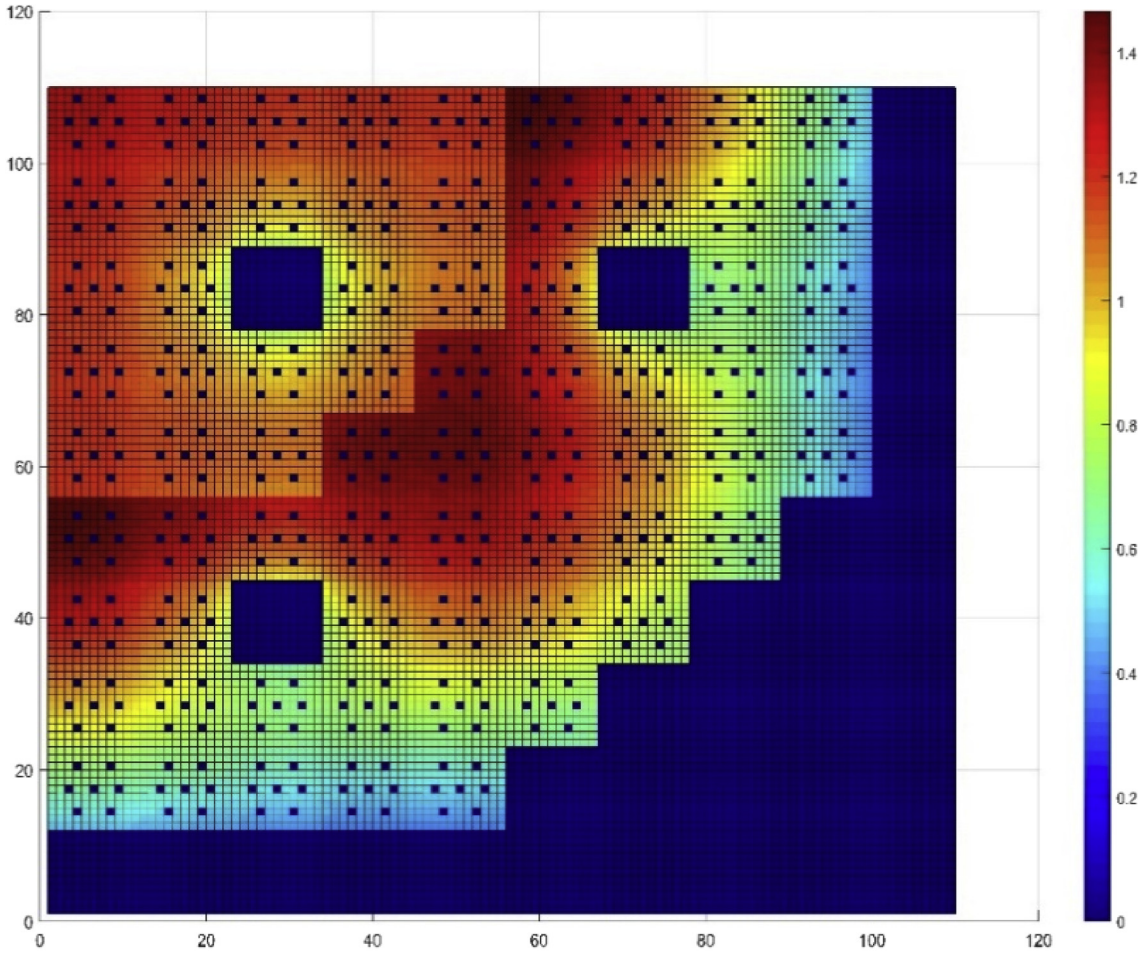

Fig. 14. Pin-wise power distribution obtained with MCS.

For the Case A nominal state, although 33G calculation introduces −312 pcm differences in the k_{eff} value, the pin-wise power distribution has good agreement compared to the MCS reference solutions (Fig. 18). The RMS of the relative difference on pin-wise power distribution is 2.09%. By increasing the energy group number to 195 groups, the accuracy is improved by 177 pcm. The relative differences in pin-wise power distribution are also reduced so that its RMS is only 0.96%.

Since 15 Control Rod assemblies were loaded in Case B, the power was concentrated in the center of the core. The gradient of power from the inner core to outer core became large. Although the 33G calculation of Case B nominal state only has a difference of −39 pcm, it is believed that the error cancellation occurred in this case. According to Fig. 19, the RMS is 3.26% and the minimum value reaches −7.31%. For the other two cases, the 33G calculation has a difference of 100 pcm in the k_{eff} value and around 3% in the RMS value. In order to improve the accuracy, the 195G calculations were performed. The result of the 195G calculation are around 100 pcm bigger than that of 33G calculation. Compare to the reference solutions, the differences in the k_{eff} value of the three cases are less than 65 pcm and the RMS value of the pin-wise power distribution of each case are less than 2%.

6. Conclusions

In order to perform fast reactor whole-core analysis, the STREAM code has been coupled with the TULIP code to perform such calculations in this paper. In the coupled code system, the TULIP code calculates self-shielded cross-sections and the STREAM code performs 2-D MOC whole-core transport calculation. To verify the coupled code system, a set of assembly and core problems were calculated while the references were obtained with a MCS Monte Carlo simulation.

The sensitivity studies based on PASCAR assembly design were performed first to investigate the factors that affect the accuracy. According to the numerical results, the ring-wise model for cross-sections generation obtains more accurate results than the type-wise model. 195-group and transport correction approximation were implemented to reduce the memory and computational time, which had little effect on the final results.

Then, two more pseudo 2-D core problems were analyzed. One was based on the PASCAR core design with rectangular assembly, while the other one was based the MET-1000 core design with a hexagonal assembly. Compared to the references, a more detailed model of non-fuel assembly would improve the results, especially the assembly- and pin-wise power distribution. For the problem of the PASCAR core, the relative differences in the k_{eff} value were less than 200 pcm in both the no-CR-assembly case and CR-assembly case. The RMS differences on pin-wise power were 0.27% and 0.32%, respectively. According to the results of the MET-1000 core, 33-group calculations obtained the k_{eff} value with 300 pcm differences and 3.26% RMS value of pin-wise power distribution, which is acceptable. Compared to the results of 33-group calculations, the 195-group calculations significantly improved the accuracy, especially for the pin-wise power distribution. For each verification case, the differences of the k_{eff} value were less than 100 pcm and the

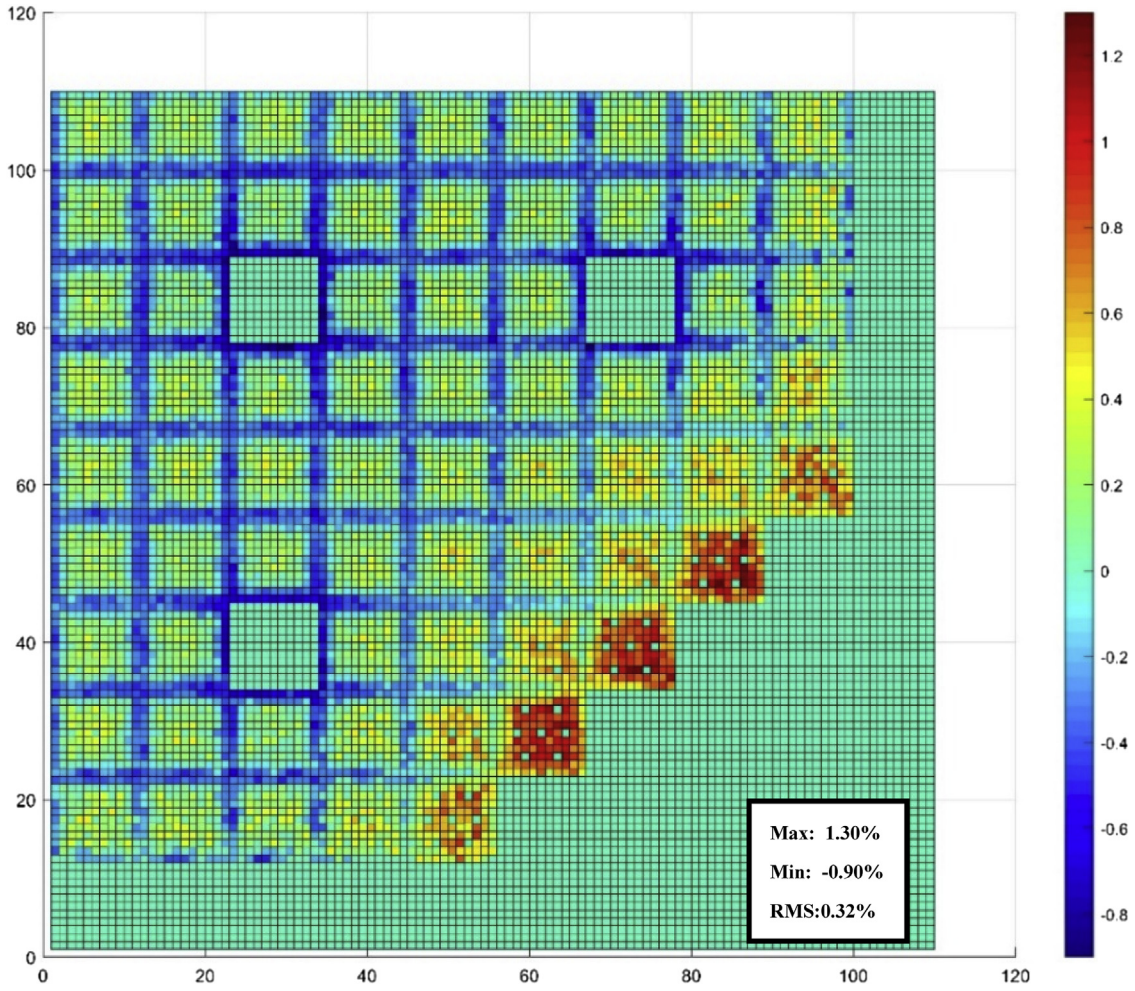

Fig. 15. Relative difference of pin-wise power distribution, unit in %.

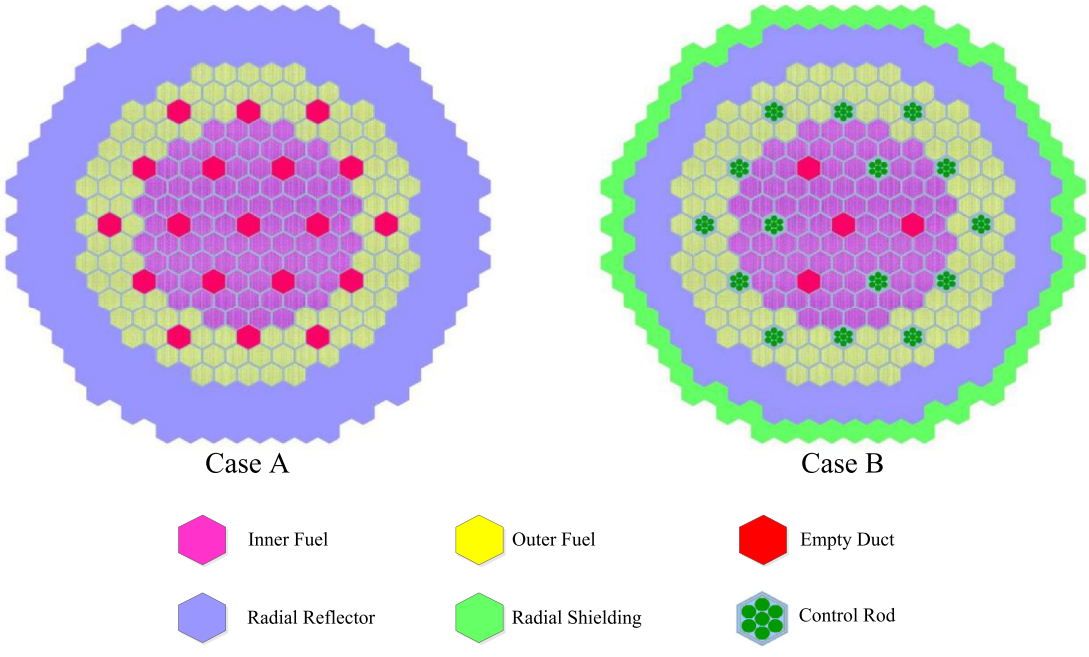

Fig. 16. Layout of Case A and Case B 2-D MET-1000 core problems.

Table 8
Summary of k_{eff} value of each case.

Case	Code	k_{eff}	Diff., pcm
Case A nominal	MCS	1.23895 ± 0.00003	
	TULIP/STREAM, 33G	1.23418	−312
	TULIP/STREAM, 195G	1.23687	−135
Case B nominal	MCS	1.05816 ± 0.00003	
	TULIP/STREAM, 33G	1.05772	−39
	TULIP/STREAM, 195G	1.05889	65
Case B SV	MCS	1.09700 ± 0.00003	
	TULIP/STREAM, 33G	1.09585	−96
	TULIP/STREAM, 195G	1.09735	29
Case B Doppler	MCS	1.05657 ± 0.00003	
	TULIP/STREAM, 33G	1.05538	−106
	TULIP/STREAM, 195G	1.05659	2

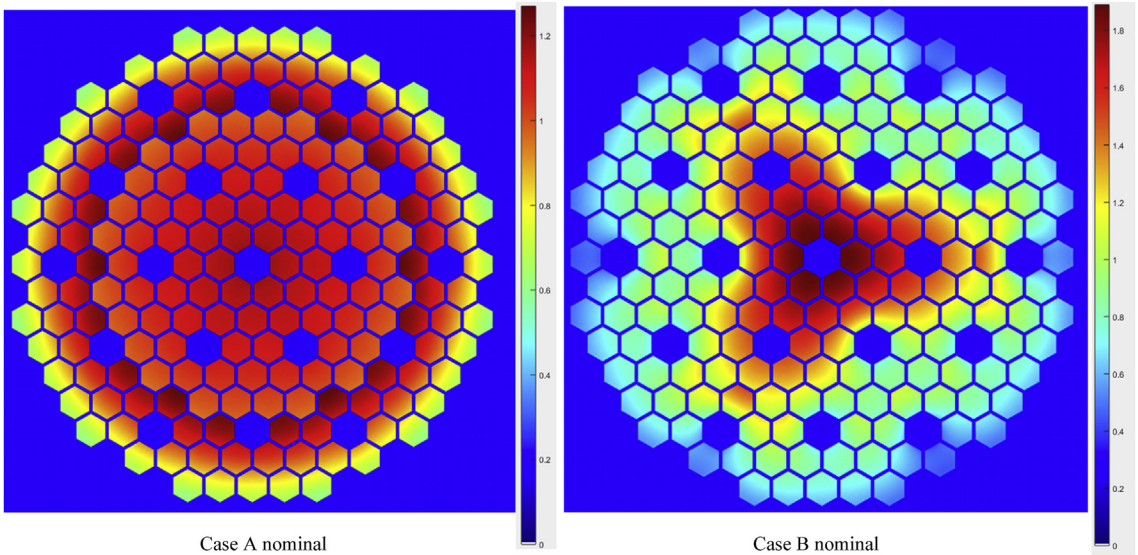

Case A nominal
Max. 1.120
Min. 0.611

Case B nominal
Max. 1.890
Min. 0.436

Fig. 17. Reference relative pin-wise power distribution of Case A and Case B nominal state.

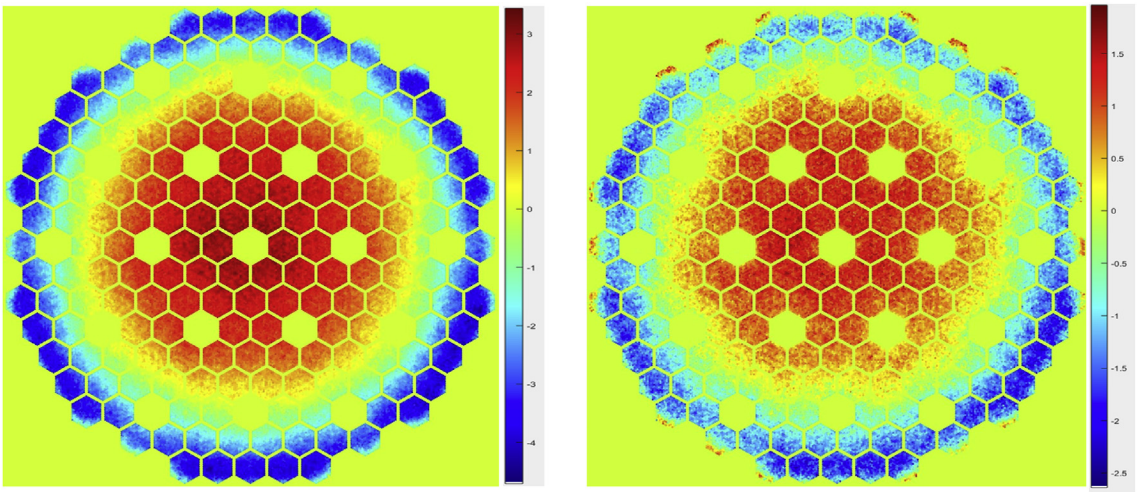

Case A – 33G
Max. 3.44%
Min. -4.71%
RMS 2.09%

Case A – 195G
Max. 1.96%
Min. -2.64%
RMS 0.96%

Fig. 18. Relative difference on pin-wise power distribution of Case A nominal state, unit in %.

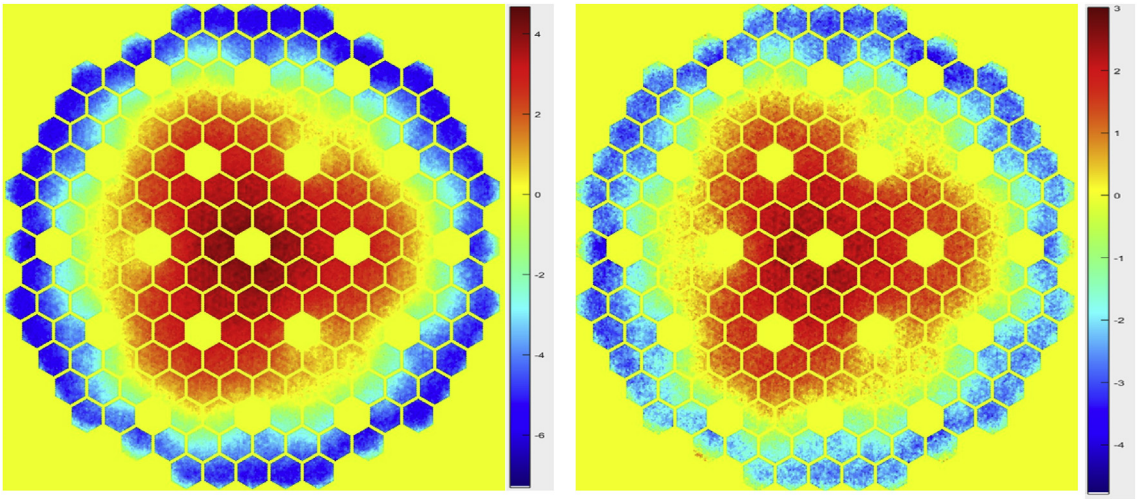

Case B – 33G
Max. 4.67%
Min. -7.31%
RMS 3.26%

Case B – 195G
Max. 3.01%
Min. -4.76%
RMS 1.76%

Fig. 19. Relative difference on pin-wise power distribution of Case B nominal state, unit in %.

Table 9
Relative difference on pin-wise power distribution of Case B SV and Doppler state.

	Group	Max.	Min.	RMS
Case B SV	33G	4.25%	−5.62%	2.85%
	195G	3.00%	−3.80%	1.65%
Case B Doppler	33G	4.21%	−6.41%	3.11%
	195G	2.58%	−3.96%	1.63%

RMS values were less than 2%.

To sum up, it was successfully verified that the coupled TULIP/STREAM code system can provide accurate results with high-fidelity resolution. In the future, the study will focus on the 3-D whole-core calculation by using MOC transport solver with explicit geometry modeling.

Acknowledgements

This work was partially supported by the National Research Foundation of Korea (NRF) grant funded by the Korea government (MSIT), (No.NRF-2017M2A8A2018595); This work was partially supported by a National Research Foundation of Korea (NRF) grant funded by the Korean government (MSIT), (No. NRF-2012M2A8A2025624); This work was supported by the National Research Foundation of Korea (NRF) grant funded by the Korea government (MSIT), (No. NRF-2019M2D2A1A03058371).

References

[1] N.Z. Cho, G.S. Lee, C.J. Park, Fusion of method of characteristics and nodal method for 3-d whole core transport calculation, Trans. Am. Nucl. Soc. 86 (2002) 322–324.
[2] J.Y. Cho, J.S. Song, K.H. Lee, Three dimensional nuclear analysis system DeCART/CHORUS/MASTER, in: ANS Annual Meeting, Atlanta, USA, June 16–20, 2013.
[3] Y.S. Jung, C.B. Shin, C.H. Lim, H.G. Joo, Practical numerical reactor employing direct whole core neutron transport and subchannel thermal/hydraulic solvers, Ann. Nucl. Energy 62 (2013) 357–374.
[4] B. Collins, S. Stimpson, B.W. Kelley, M.T. Young, B. Kochunas, A. Graham, E.W. Larsen, T. Downar, A. Godfrey, Stability and accuracy of 3D neutron transport simulations using the 2D/1D method in MPACT, J. Comput. Phys. 326 (2016) 612–628.
[5] J. Chen, Z.Y. Liu, C. Zhao, Q.M. He, T.J. Zu, L.Z. Cao, H.C. Wu, A new high-fidelity neutronics code NECP-X, Ann. Nucl. Energy 116 (2018) 417–428.
[6] S. Choi, C. Lee, D. Lee, Resonance treatment using pin-based pointwise energy slowing-down method, J. Comput. Phys. 330 (2017) 134–155.
[7] S. Santandrea, L. Graziano, D. Sciannandrone, Accelerated polynomial axial expansions for full 3D neutron transport MOC in the APOLLO3® code system as applied to the ASTRID fast breeder reactor, Ann. Nucl. Energy 113 (2018) 194–236.
[8] C.H. Lim, H.G. Joo, W.S. Yang WS, Development of a fast reactor multigroup cross section generation code EXUS-F capable of direct processing of evaluated nuclear data files, Nucl Eng Technol 50 (2018) 340–355, v3.
[9] C.H. Lee, W.S. Yang, MC2-3: multigroup cross section generation code for fast reactor analysis, Nucl. Sci. Eng. 187 (2017) 268–290.
[10] W.S. Yang, M.A. Smith, C.H. Lee, A. Wollaber, D. Kaushik, A.S. Mohamed, Neutronics modeling and simulation of SHARP for fast reactor analysis, Nucl Eng Technol 42 (v5) (2010) 520–545.
[11] S. Choi S, D. Lee. Efficient parallelization strategy of STREAM for three-dimensional whole-core neutron transport calculation, in: Transactions of the Korean Nuclear Society Spring Meeting, Jeju, Korea, May 17-18, 2018.
[12] K. Kim, S. Choi, D. Lee. Validation of ultra-fine group library generation of lead-cooled fast reactor for STREAM code. In Transactions of the Korean Nuclear Society Spring Meeting, Jeju, Korea, May 17-18, 2018.
[13] X.N. Du, L.Z. Cao, Y.Q. Zheng, H.C. Wu, A hybrid method to generate few-group cross sections for fast reactor analysis, J. Nucl. Sci. Technol. 55 (v8) (2018) 931–944.
[14] Y.Q. Zheng, X.N. Du, Z.T. Xu, S.C. Zhou, Y. Liu, C.H. Wan, L.F. Xu, SARAX: a new code for fast reactor analysis part I: Methods, Nucl. Eng. Des. 340 (2018) 421–430.
[15] Y.Q. Zheng, L. Qiao, Z.A. Zhai, X.N. Du, Z.T. Xu, SARAX: a new code for fast reactor analysis part II: verification, validation and uncertainty quantification, Nucl. Eng. Des. 331 (2018) 41–53.
[16] C. Steven, V.D. Marck, Benchmarking ENDF/B-VII.0, Nucl. Data Sheets 107 (2006) 3061–3118.
[17] T. Tone, A numerical study of heterogeneity effects in fast reactor critical assemblies, J. Nucl. Sci. Technol. 12 (v8) (1975) 467–481.
[18] R.E. MacFarlane, D.W. Muir, A.C. Kahler, The NJOY Nuclear Data Processing System, Version 2012, Los Alamos National Laboratory, New Mexico, 2012. LA-UR-12-27079.
[19] A. Yamamoto, M. Tabuchi, N. Sugimura, T. Ushio, M. Mori, Derivation of optimum polar angle quadrature set for the method of characteristics based on approximation error for the bickley function, J. Nucl. Sci. Technol. 44 (v2) (2007) 129–136.
[20] J.Y. Cho, K.S. Kim, H.J. Shim, J.S. Song, C.C. Lee, H.G. Joo, Whole core transport calculation employing hexagonal modular ray tracing and CMFD formulation, J. Nucl. Sci. Technol. 45 (v8) (2008) 740–751.
[21] J.R. Jang, W.Y. Kim, S.G. Jeong, E. Jeong, J.S. Park, M. Lemaire, H.S. Lee, Y.M. Jo, P. Zhang, D. Lee, Validation of UNIST Monte Carlo code MCS for criticality safety analysis of PWR spent fuel pool and storage cask, Ann. Nucl. Energy 114 (2018) 495–509.
[22] S.Y. Choi, J.H. Cho, M.H. Bae, J. Lim, D. Puspitarini, J.H. Jeun, H.G. Joo, S. Hwang, PASCAR: long burning small modular reactor based on natural circulation, Nucl. Eng. Des. 241 (v5) (2011) 1486–1499.
[23] OECD/NEA, Benchmark for Neutronic Analysis of Sodium-Cooled Fast Reactor Cores with Various Fuel Types and Core Sizes, vol. 9, NEA/NSC/R, 2015.